QUARTERLY JOURNAL OF THE ROYAL METEOROLOGICAL SOCIETY
Q. J. R. Meteorol. Soc. **133**: 1087–1100 (2007)
Published online in Wiley InterScience
(www.interscience.wiley.com) DOI: 10.1002/qj.109

RMetS
ROYAL METEOROLOGICAL SOCIETY

Modelling suppressed and active convection. Comparing a numerical weather prediction, cloud-resolving and single-column model

J. C. Petch[a]*, M. Willett[a], R. Y. Wong[a] and S. J. Woolnough[b]
[a] *Met Office, Exeter, UK*
[b] *The Walker Institute, Department of Meteorology; University of Reading, UK*

ABSTRACT: This paper describes the design of and basic results from a case study to compare simulations of convection over the Tropical West Pacific. Simulations are carried out using a cloud-resolving model (CRM), a global numerical weather prediction (NWP) model and a single-column version of the NWP model (SCM). The experimental design for each model type is discussed and then results are compared. The periods simulated each include a regime with strong convective activity, a much more suppressed regime with far less convection, as well as the transition between these regimes. The description of the design and basic results from this study are given in some detail, as a study including all these model types is relatively new. Comparing the local forcing due to the dynamics in the NWP model with the observed forcing used to drive the CRM and SCM it is found that there is good agreement for one period chosen but significant differences for another. This is also seen in fields such as rain rate and top-of-atmosphere radiation. Using the period with good agreement we are able to identify examples of biases in the NWP model that are also reproduced in the SCM. Also discussed are examples of biases in the NWP simulation that are not reproduced in the SCM. It is suggested that understanding which biases in the SCM are consistent with the full NWP model can help focus the use of an SCM in this framework. © Crown Copyright 2007. Reproduced with the permission of the Controller of HMSO. Published by John Wiley & Sons, Ltd

KEY WORDS convection; forecasts; GCSS

Received 13 December 2006; Revised 1 May 2007; Accepted 3 May 2007

1. Introduction

This paper describes the advancement of an experimental framework typically used by some of the working groups of the GEWEX (Global Energy and Water Cycle Experiment) Cloud System Study (GCSS). The purpose of the GCSS is to support the development of new parametrizations of all cloud-related processes for large-scale models (Randall *et al*., 2000). The work presented here most closely relates to the GCSS precipitating cloud systems working Group (PCSWG), which specifically aims to support the development of the parametrization of precipitating convective cloud systems in global climate models and numerical weather prediction (NWP) models. This has typically been done through a comparison of various different single-column models (SCMs) and cloud-resolving models (CRMs). The resulting collaboration and the papers describing these cases provide a testbed for various institutions to carry out further experiments using these cases. Other benefits of this type of intercomparison work and its publication are:

- the experimental design and basic behaviour of various models are available in the literature for reference
- model errors can be identified as either a community-wide problem or a specific model problem, and tackled in the appropriate way
- a typical magnitude of spread between models for a given diagnostic can be identified
- errors in model set up can be identified more easily than if only one institution has carried out a simulation.

The previous intercomparison work of the GCSS PCSWG has covered a range of convective situations including a tropical oceanic squall line (Redelsperger *et al*., 2000; Bechtold *et al*., 2000), summertime convection over the central US (Xu *et al*., 2002; Xie *et al*., 2002) and the development of convection over tropical land (Grabowski *et al*., 2005). The choice of each case is typically motivated by what are considered the current major problems in climate and NWP models, although it is also influenced by the availability of data suitable for driving SCMs and CRMs as well as any specific drives by funding bodies.

It has been recognised for many years that the parametrization of the major physical processes related to deep tropical convection are critical in global models and so there has often been a focus on the tropics in convective development work (e.g. Gregory and Miller, 1989).

* Correspondence to: J. C. Petch, Met Office, FitzRoy Road, Exeter, EX1 3PB, UK. E-mail: jon.petch@metoffice.gov.uk

The GCSS PCSWG has also focused on tropical convection in the past, with its first case (Redelsperger *et al*., 2000) and an unpublished second case both focused on convection over the Tropical West Pacific (TWP). While the second case was not published, it did spawn a range of sensitivity studies from those involved (e.g. Wu *et al*., 2000; Petch and Gray, 2001).

Previous studies by the GCSS PCSWG over the TWP have tended to be dominated by very active periods of convection. The case discussed in this paper focuses on both suppressed and active periods of tropical convection. Weaknesses in the representation of periods of suppressed convection have previously been identified as having a detrimental effect on simulations of sub-seasonal variability in tropical convection, and in particular the poor representation of the Madden-Julian Oscillation by climate models. For example, Inness *et al*. (2001) demonstrated that increased vertical resolution led to an improved simulation of the Madden-Julian Oscillation in HadAM3 (an earlier version of the Met Office Unified Model). This was shown to be linked to an improved representation of the freezing level inversion and an increase in the amount of convection with tops around the freezing level, and moistening by these clouds. More recently, Grabowski (2003) has attributed the strong intraseasonal variability in an aquaplanet simulation with 'cloud-resolving convective parametrization' (CRCP) to a greater sensitivity of convection to the moisture profile in the CRCP than in conventional parametrization schemes, and the important role of moistening of the profile by convection during the transition from suppressed to active convection. The importance of the more suppressed periods of convection is also backed up by observations. For example, Lin and Johnson (1996) identified periods of significant moistening by convection during the suppressed periods of TOGA-COARE and Johnson *et al*. (1999) highlighted the prevalence of cumulus and cumulus congestus clouds at these times and associated these clouds with this moistening.

As well as moving the focus of this work to include less active periods of tropical convection, another new and key component of this work is to include an NWP model. Randall *et al*. (1996) described in detail the framework for combining SCMs, CRMs and observations for developing global models. Here, we build on this framework by including the analysis of an NWP model in the same way as the SCM (i.e. focusing on the column properties over a single region for the same period) which allows us to better understand the relevance of biases seen in the SCM. If a bias is defined as a significant difference between the SCM or NWP model and observations (or the CRM) then there are two possible bias outcomes from this experimental framework. They are:

- the SCM and NWP model exhibit a similar bias; referred to as a *type S* bias
- the SCM and NWP model do not exhibit a similar bias; referred to as a *type D* bias.

The definition of what a 'significant' bias is, and if the bias is 'similar' in the NWP model and SCM is subjective. However, the concept of these bias types is a useful one as it can give us some insight into which NWP biases can be easily studied using the SCM. This type of thinking, along with separating out different reasons why the SCM and NWP model may not exhibit a similar bias, can also help us begin to interpret other implications of this experimental framework; this is summarized in Table I. It is also the case that biases seen in NWP simulations often link strongly to errors in full climate models (e.g. Klein *et al*., 2006) so the framework used in this paper is also of relevance for climate models.

This paper presents the results from simulations of convectively active and suppressed periods over the TWP using the Met Office SCM, CRM and NWP model. To the authors' knowledge, this is the first report involving simulations of convection in the TWP using a CRM, an SCM and a full NWP model analysed in this way. It describes how the case was designed, how the main periods were chosen and how they can be broken down into active and suppressed sub-periods. The results are discussed in terms of the biases seen in the SCM and NWP models, where possible using the framework described in Table I. Section 2 gives an overview of the experimental design, including the three models used in this study and the selection of active and suppressed periods. Section 3 compares the analysis and direct response of the NWP model to the observational-based-forcing used to drive the CRM and the SCM. Section 4 then describes example biases in the SCM and NWP models and section 5 summarises the key points from this work.

2. Experimental design

2.1. The models used in this study

Three different models have been used in this study; these are a cloud-resolving model, a global NWP model and an SCM version of an NWP model. Ongoing work (Willett, personal communication; Woolnough, personal communication) will report on comparisons between these models and the same types of model developed at other centres for this case. However, to describe the design and basic results of this experimental framework, one model of each type is sufficient.

Before describing the design of the CRM and SCM component of the experiment it is worth explaining why CRMs are a very important component of this work. Clearly observations are critical to this work because they are used to create the NWP analysis, to create the SCM and CRM forcing data and for the evaluation of the different models. However, the use of the CRM to evaluate the SCM is essential for two main reasons. Firstly, CRMs can provide information about a wide range of parameters that cannot be easily observed (e.g. convective mass flux, detailed cloud microphysical information and radiative heating profiles). Secondly, CRMs are responding to the exact same forcing as the

DOI: 10.1002/qj

Table I. Summary of the bias types we can consider in the experimental framework presented in this paper.

Bias type	Summary	Possible causes and other issues	Further comments and tests
S	There is a similar bias in SCM and NWP model. This is the most likely to be a pure *parametrization driven bias*.	The parametrizations are behaving the same in both models so the SCM is a good tool within this framework to study this bias.	Before addressing we should still consider if the bias in question is linked to a significant problem with the full NWP model.
D1	There is a bias in SCM but not in the NWP model. This is likely to be due to *a lack of dynamical feedback* in the SCM.	SCM has formed unphysical profiles (and not typical of the full model) due to lack of dynamical feedback.	The SCM can be kept closer to physically realistic profiles by re-initialising more frequently and running for shorter periods.
		SCM has a bias due to deficiencies with the parametrizations but this is manifested differently in the NWP model due to dynamical feedbacks.	It may be useful to address this bias in the SCM if we can link it to a known deficiency with the parametrization or a bias in the full model. However, making a link to a bias in the full model may be difficult.
D2	There is a bias in NWP model but not in the SCM. This is most likely linked to *initial conditions and forcings used*.	NWP bias is due to analysis (e.g. ERA40) differing significantly from the observations.	Run NWP model with a different analysis and/or consider sensitivity of parametrizations to initial conditions using SCM studies.
		NWP error is formed through the feedback of parametrization errors on the large-scale dynamics.	Could be a local or non-local problem with the physics, manifested in a different way to the SCM due to lack of dynamical feedbacks in the SCM.

SCM, whereas observations, due to a lack of temporal and spatial sampling, can have significant inconsistencies between the evaluation fields and the forcing data. Therefore when considering a bias in the SCM, it is always worth using the CRM as a reference state as well as observations when they are available.

The CRM used is based on the Met Office Large Eddy Model first described in Shutts and Gray (1994) and more recently in Petch and Gray (2001). It includes a five-category prognostic microphysical scheme (Swann, 1998; Brown and Heymsfield, 2001) which has been run with prognostic variables for both mass and number concentration of ice. The subgrid turbulence scheme is based on the Smagorinsky-Lilly model and is essentially a three-dimensional version of a first-order mixing-length closure (see Brown *et al*., 1994 for further details). There is no explicit diffusion apart from that given by the sub-grid model, although a third-order advection scheme is used for scalars and this leads to some dissipation of scalar variance. The radiation scheme included in the model is described in Edwards and Slingo (1996) and its configuration in the CRM is given in Petch and Gray (2001).

For the main simulations the CRM has been run in 2D with a horizontal domain of 525 km and a horizontal grid length of 350 m. A vertical domain of 20 km is used with the number of vertical levels chosen to give a vertical grid length of 250 m in the free troposphere stretched to give shorter grid lengths in the lowest 2 km. The top 5 km of the grid includes a damping layer to absorb gravity waves and for any run the initial temperature in the lowest 200 m is modified to include a random perturbation with a maximum amplitude of 0.25 K. The sensitivity of the CRM results to the domain size, resolution and the use of 2D or 3D is always a key question to ask when designing a framework such as this. While this has been tested, the detail of the results is beyond the scope of this paper. However, it should be noted that for the results presented in this paper, the biases or features seen in comparisons between the SCM and the CRM were robust across all reasonable CRM domain sizes, resolutions and in 2D and 3D.

The NWP model is the global forecast version of the Met Office's Unified Model (UM) that was used operationally between January and December 2005. The model shares its dynamics and physics with the atmospheric component of the Hadley Centre Global Environment Model (HadGEM1). The dynamics is a two-time level, semi-implicit, semi-Lagrangian formulation and is non-hydrostatic. The physics schemes are basically the same as those described for HadGEM1 (Martin *et al*., 2005). The horizontal resolution is 0.83 degrees longitude by 0.56 degrees latitude (90 km by 60 km on the equator). There are 38 levels in the vertical with the model top at around 3 hPa. The dynamics and physics schemes all use a time step of 20 minutes except for the radiation scheme, which uses a 3 hour time step, and the convection scheme, which uses a 10 minute time step.

For this work the model was initialised from ERA-40 (Uppala *et al*., 2005); this was considered the best analysis available for this period, given that it would be

DOI: 10.1002/qj

used to initialise a range of global models as part of the multi-model comparison work. Forecasts were run for 48-hours from 0Z on every day and concatenated together to form a single continuous forecast for each period using either the 0–24 hour forecast or the 24–48 hour forecast. For the comparison with observations, analysis was carried out on the mean of all the points that lie within the IFA; with the current forecast resolution, this means the values shown in this paper are the average of 20 grid points.

The SCM is a single column version of the NWP model. For total consistency, it includes identical parametrizations to the full NWP model and is run with the same time step and vertical resolution. The use of an SCM with a different time step or resolution to the NWP model is only of value as part of a sensitivity study aiming to understand the behaviour of the parametrizations.

2.2. Choosing the periods for this study

The focus of this experiment is the modelling of the atmosphere over the tropical ocean for periods of suppressed and active convection including the transition between these states. We have chosen to use a selection of periods from TOGA-COARE (Tropical Ocean Global Atmosphere-Couple Ocean Atmosphere Response Experiment) (Webster and Lukas, 1992). TOGA-COARE was a field experiment that provides suitable observations and forcing data from a region of the TWP for a four-month period beginning 1 November 1992. Observations taken during TOGA-COARE have been processed to provide appropriate forcing for an SCM or CRM by Ciesielski *et al*. (2003). The observations were focused on the TOGA-COARE intensive flux array (IFA), a region of about 400 km by 250 km centred on 2 °S 155 °E.

For this study, it was decided to focus on some shorter periods from the full four months of TOGA-COARE; the length of these was a balance between having a suitable averaging period for the data and the computational expense involved in the NWP and CRM runs. Periods have been chosen such that each begins with some deep convective activity, then has a phase of mostly suppressed convection and finally a period of more active convection. The active period at the start was useful to ensure that the CRM generated horizontal variability associated with deep convection before the start of the suppressed period. Surface rain rate was the main diagnostic used to define what was active and suppressed. Periods were chosen using the observations made during TOGA-COARE and some 2D, small domain (256 km), large grid-length (1 km) CRM experiments were driven by these observations.

Figure 1 shows rain rate and precipitable water derived from observations taken during the four months of TOGA-COARE and from the four, one-month duration CRM simulations. Highlighted on this plot are three

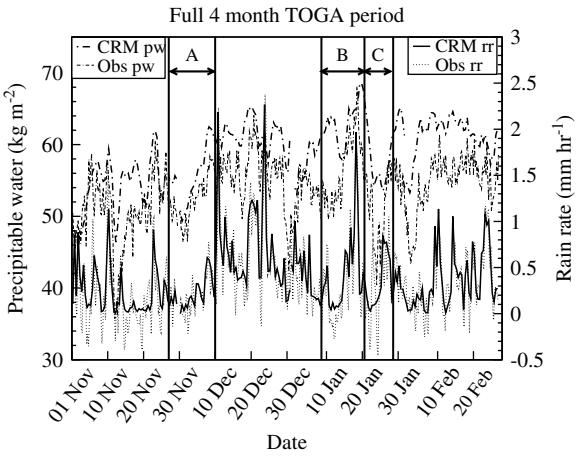

Figure 1. Time series or 12-hourly mean values of precipitable water (pw) and rain rate (rr) from the full four months of TOGA-COARE. Shown are results from CRM simulations initialised at the start of each month and values based on observations. The rain rate (obs rr) is derived from the moisture budget. Highlighted on the plot are the three periods chosen for this study.

periods that exhibit the desired active and suppressed behaviour in rainfall; they are: A (0Z 28 Nov to 0Z 10 Dec 1992); B (0Z 9th Jan to 0Z 21 Jan 1993) and C (0Z 21 Jan to 0Z 29th Jan 1993). Periods B and C will be considered further in this study as these involved NWP simulations. Period A is shown here only for completeness as it was simulated by SCM and CRMs as part of the GCSS multi-model comparison. It is also worth noting that other options are available from the four months that had suppressed followed by active convection such as the dry intrusion in mid-November (studied by Redelsperger *et al*., 2002) but the periods chosen are representative, with period B including some of the period described as suppressed by Wu *et al*. (2000).

A further point to note from Figure 1 is that there are significant differences between the observed and CRM precipitable water. While this could be related to problems with the CRM simulations, it is far more likely that differences of this size are due to deficiencies in the forcing data because the observations were not of sufficient temporal or spatial resolution to have well balanced moisture (or heat) budgets. This also explains why the rain rates derived from the budget study often have negative values. This issue of inconsistencies in the forcing has been raised in the past and is discussed in more detail in Wu *et al*. (2000). It is possible to force a moisture balance using variational analysis techniques such as those used by Zhang and Lin (1997), but for this case, with the version available at the time, the modified forcing data led to a less realistic simulation with the CRM (Zhang, personal communication). A final point to note is that some of the large discrepancies between the CRM and observed precipitable water are due to the long integrations carried out in the CRM; these are significantly smaller in the CRM runs of the chosen periods.

DOI: 10.1002/qj

3. Comparing the observational based forcing with the NWP model

3.1. Initial conditions

The basic design of the SCM and CRM experiments follows the methods of most of the previous GCSS PCSWG experiments (e.g. Xu *et al*., 2002), while the NWP model is initialised at 0Z daily from ERA-40. The initial values of potential temperature and moisture taken at the start of the two periods are shown in Figure 2a and the observed sea surface temperatures (SSTs) acting as the lower boundary condition in the SCM and CRM are shown in Figure 2b. For clarity the initial conditions are plotted for the lowest 8 km only; above this there was little moisture and there were no significant features in the temperature profiles to discuss. From Figure 2a it can be seen that the initial temperatures used for both cases are within a degree of each other with case C slightly warmer. The initial water vapour profiles for case C are significantly more moist than case B through most of the profile; this is especially noticeable around 5 km. Also included in Figure 2b are the SST values averaged over the IFA that are used in the NWP model; these are from the Met Office GISST 2.0 dataset. It can be seen from Figure 2b that the SSTs used in the NWP model are essentially a monthly mean so there is no representation of the SST variability on diurnal or longer timescales that is seen by the CRM and SCM.

As the NWP model is initialised every day, it is useful to know the temperatures and water vapour profiles in the analysis through the whole period and to have an idea of how this compares with the observations used to derive the forcing for the SCM and CRM. This is best shown as a time-height contour plot of the difference between the ERA-40 value used in the NWP model and the observed values. Figure 3 shows this difference for water vapour and potential temperature throughout both periods B and C along with the mean values for both periods. A key point to note from these plots is that there is a significant difference in the water vapour content for period C with the analysis being significantly drier; this is not the case during period B. There are no strong signals in the potential temperature although the analysis appears to be generally slightly cooler than the observations. The implications of the drier analysis than observation for case C are significant and will be discussed the following section.

3.2. Dynamical forcing and the hydrological cycle

The CRM and SCM are forced using profiles of large-scale temperature and moisture tendencies derived from the six-hourly observations (Figure 4). The horizontal winds are relaxed back to the observed values (not shown) with a two-hour time scale. From Figure 4 it is clear that during the latter part of both periods there is significant large-scale cooling and moistening in the forcing data. This is what drives the most active convection. This cooling and moistening becomes most notable after 144 hours in period B and 120 hours in period C, with period B having the strongest forcing. During the middle periods of both cases the forcing is generally weak with small amounts of warming and drying at some of the times.

On a time-scale of a day or more it is known that rain rate and precipitable water in CRM simulations are strongly constrained by the forcing applied; this is also true of clouds to some extent although they can show more variability (e.g. Xu *et al*., 2002). Figure 5 shows time series of rain rate, precipitable water, cloud fraction and cloud centre of mass (this is a measure of cloud height and is defined in Grabowski *et al*., 2005) from CRM simulations of periods B and C. Also shown on these plots and summarised in Table II are sub-periods, which are classed as suppressed and active. The definitions of these sub-periods are somewhat arbitrary but they do allow us to investigate the response of parametrizations in quite different situations and aid in the discussion of results. Working in whole days, the suppressed periods generally have a rain rate of less than 0.2 mm hr^{-1} and a cloud fraction less than 20%, and the active periods have values larger than this; the first 48

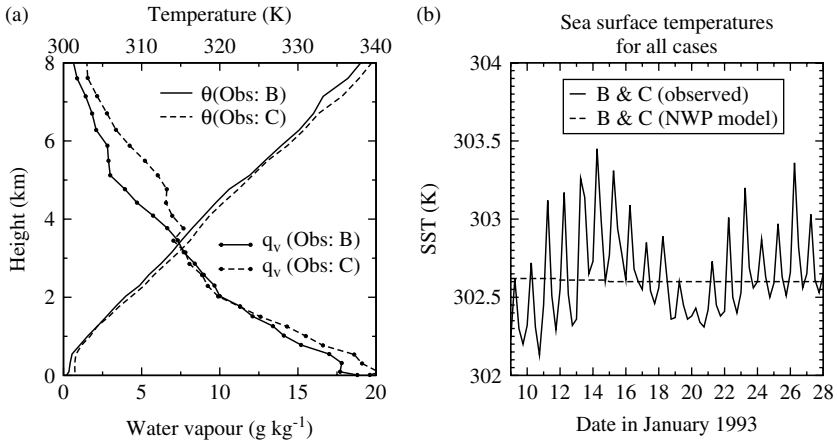

Figure 2. Experimental set up for cases B and C. Shown are a) initial profiles of potential temperature and water vapour mass mixing ratio profile and b) time series of sea surface temperature used as a lower boundary condition.

DOI: 10.1002/qj

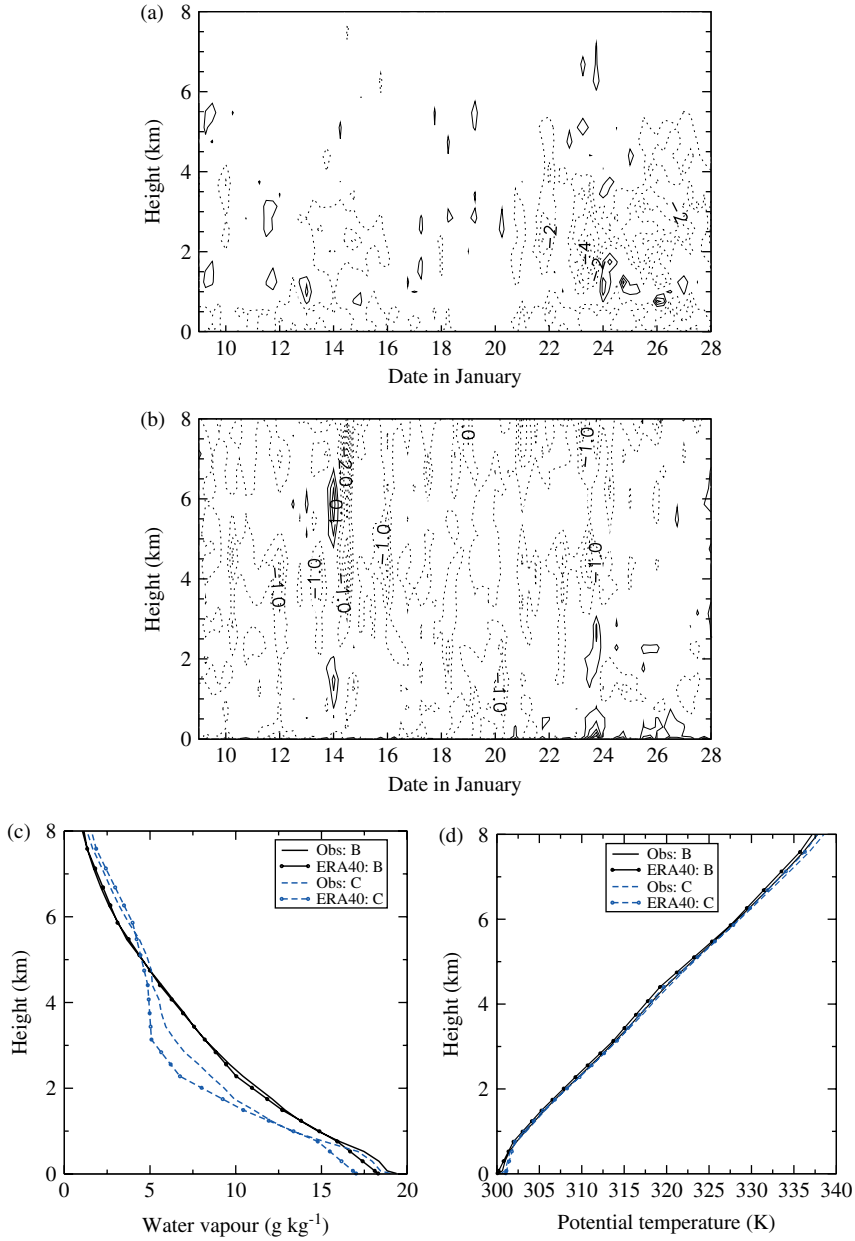

Figure 3. The upper plots show time-height contours of the difference between ERA40, which is used to initialise the NWP model, and the observations used to derive the CRM and SCM forcing. Shown is a) water vapour mixing ratio with a contour interval of 1 g kg^{-1} and b) potential temperature with a contour interval of 0.5 K. Negative contours use a dashed line. Also included are the period mean values from ERA40 and observations of c) water vapour and d) potential temperature. This figure is available in colour online at www.interscience.wiley.com/qj

hours of each case are likely to involve spin-up in the CRM and are not included.

The NWP model generates atmospheric circulations as the dynamics and physics responds to the analysis. This dynamical response leads to heat and moisture tendencies over the IFA that can be directly compared to the observational forcing used to drive the CRM and SCM. Figure 6 shows the column tendencies of temperature and moisture due to large-scale motion in the NWP model for cases B and C; these are taken from the 0–24 hour forecast period. Comparing Figure 6 with Figure 4 allows us to understand whether the physics in the NWP model is being driven in a similar way to the observations and whether the sub-periods defined in terms of the CRMs response to the observational forcing are relevant to the NWP simulations. It is clear from Figure 6 that for case B the magnitude of the tendencies are larger but the timing of suppressed and active sub-periods are close to those defined in Table II. However, as with the profiles in the analysis, period C is quite different in the NWP model from the observations with little evidence of the active sub-period in the latter part of the run. This is also clear from Table III, which shows time mean values of rain rate, top-of-atmosphere out going longwave radiation (OLR) and surface downwelling solar radiation.

Figure 7 shows time series of rain rate and precipitable water from the 0–24 hour and 24–48 hour NWP forecast; also included for reference are the values from the

DOI: 10.1002/qj

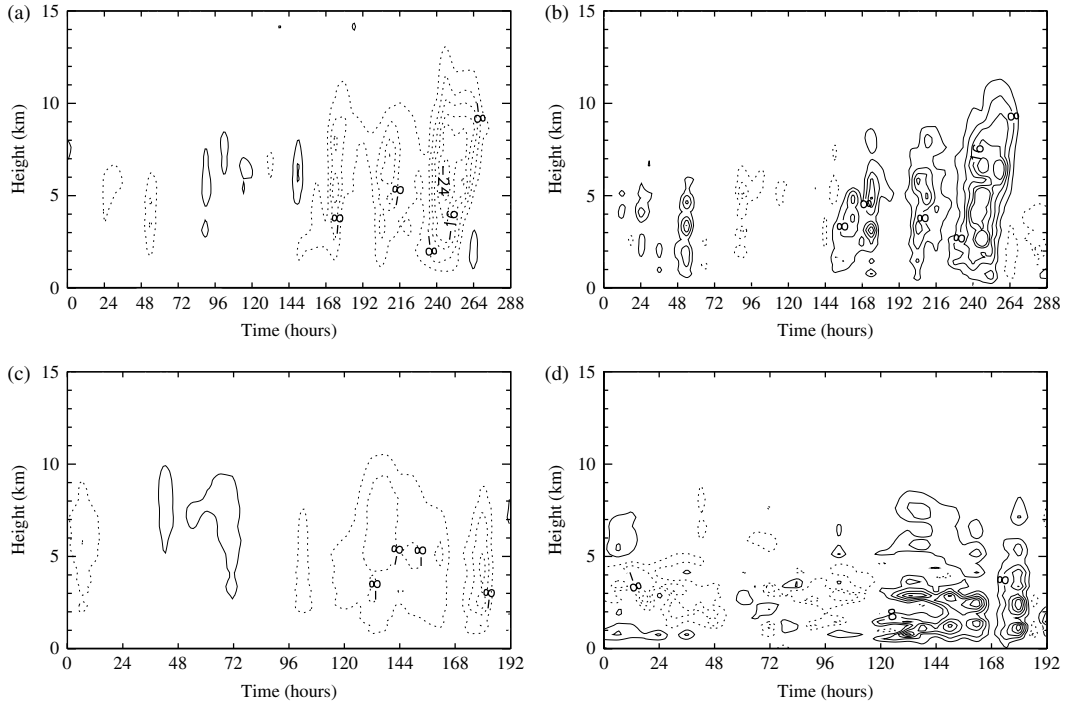

Figure 4. Large-scale forcing terms used by the SCM and CRM. These are a) temperature forcing for case B, b) moisture forcing for case B, c) temperature forcing for case C and d) moisture forcing for case C. The contour interval for all plots is 4 K day^{-1}.

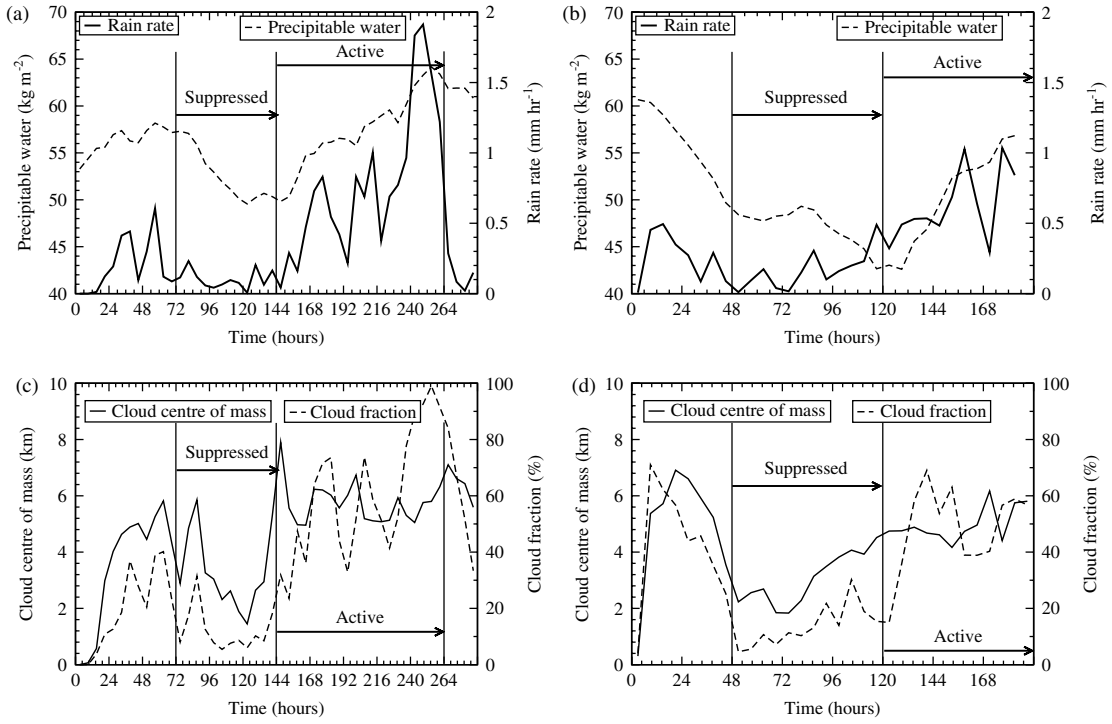

Figure 5. Time series from the CRM of six-hourly mean values of a) rain rate and precipitable water for case B, b) rain rate and precipitable water for case C, c) cloud centre of mass and cloud fraction for case B, and d) cloud centre of mass and cloud fraction for case C.

Table II. Summary of the periods chosen for this case study and the times during these classed as suppressed and active convection. Dates are for 1993 and are defined in terms of GMT.

Period	Start date	Length (hrs)	Sup (hrs)	Sup (date)	Active (hrs)	Active (date)
B	9 Jan	288	72–144	12–14 Jan	144–264	15–19 Jan
C	21 Jan	192	48–120	23–25 Jan	120–192	26–28 Jan

DOI: 10.1002/qj

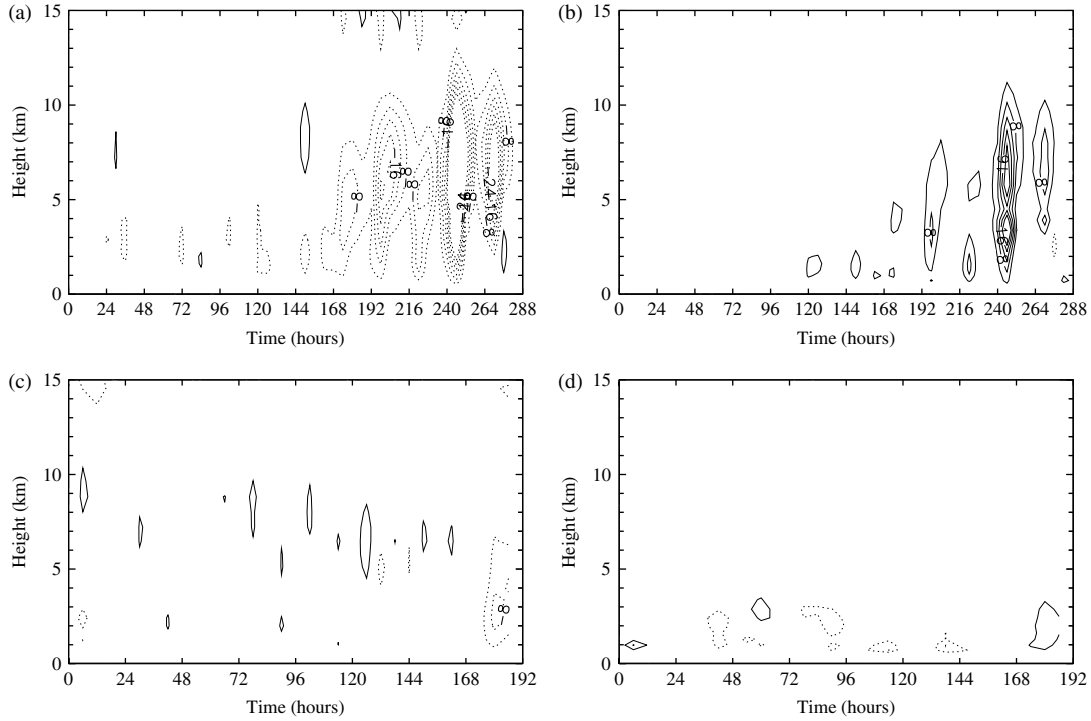

Figure 6. Tendencies of temperature (K day^{-1}) and moisture (g kg^{-1}day^{-1}) due to large-scale motion in the NWP model for cases B and C. These are a) temperature tendency for case B, b) moisture tendency for case B, c) temperature tendency for case C, d) moisture tendency for case C. The contour interval is 4K day^{-1}, which is consistent with Figure 4, however this does mean the maximum threshold is exceeded during the active period of case B.

Table III. Summary of rain rate, top-of-atmosphere out going longwave radiation (OLR) and surface downwelling solar radiation averaged during the suppressed and active periods for cases B and C. Results are shown for the CRM and the NWP model using an combined average over the 0–24 and 24–48 hour periods of the forecast cycle.

	Suppressed				Active			
	B		C		B		C	
	CRM	NWP	CRM	NWP	CRM	NWP	CRM	NWP
Rain rate (mm day^{-1})	1.8	2.5	2.3	0.1	17.8	15.4	15.1	1.8
OLR (Wm^{-2})	275	277	290	264	212	217	228	246
Surface downward solar (Wm^{-2})	313	292	319	296	239	253	278	288

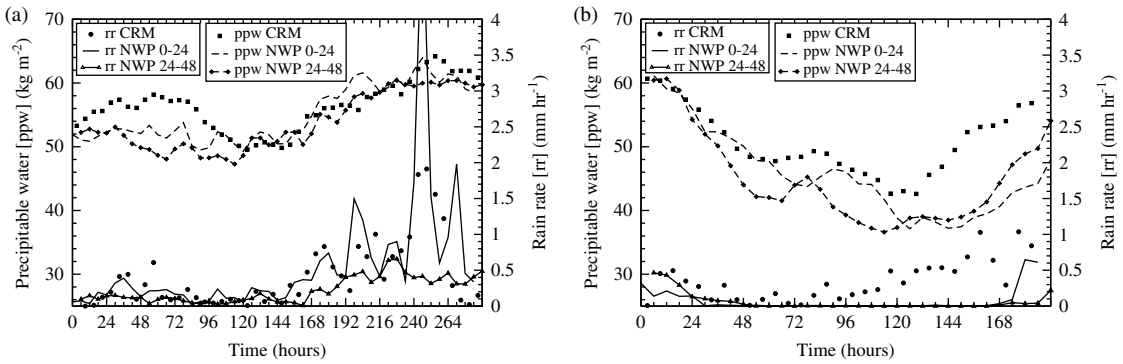

Figure 7. Time series from the NWP and CRM of rain rate and precipitable water for a) case B and b) case C.

CRM. Figure 8 shows profiles of the tendencies of temperature and large-scale water vapour averaged over the active sub-periods for the NWP forecasts along with the observational derived values. The general agreement between the NWP model dynamics and the observational forcing for case B and poor agreement for case C can be

DOI: 10.1002/qj

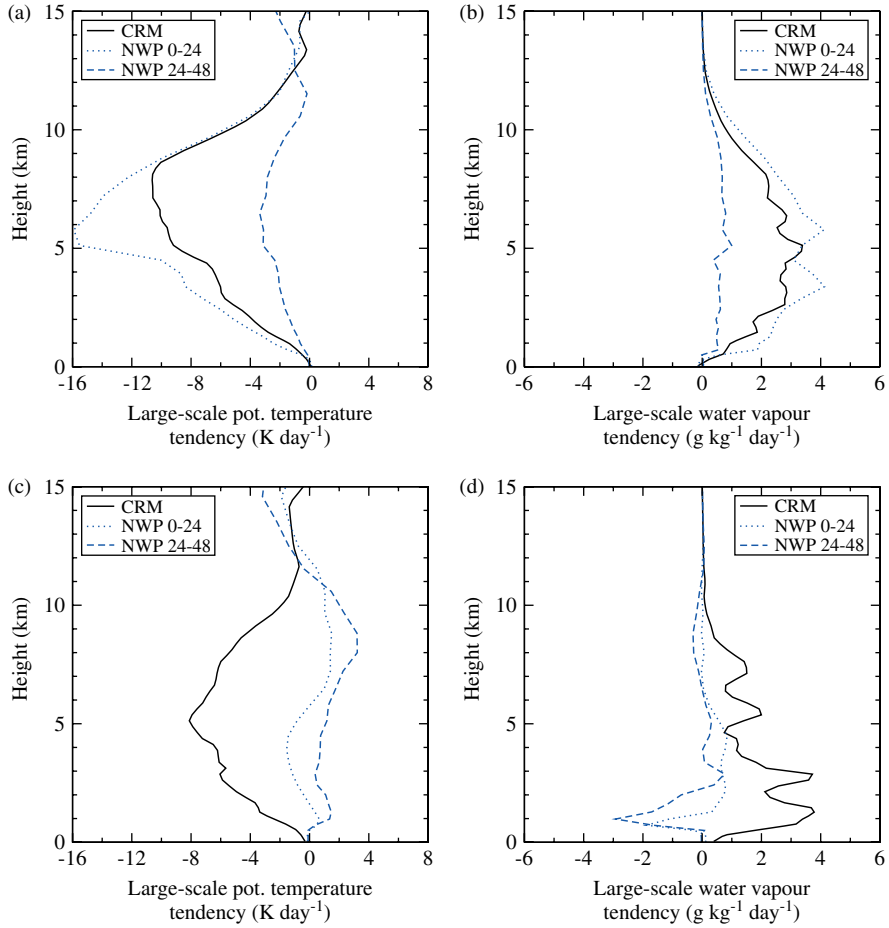

Figure 8. Profiles averaged over the active sub-periods for cases B and C defined in Table II of the NWP and observation derived large-scale tendencies of potential temperature and water vapour. Shown are a) temperature tendency for case B, b) water vapour tendency for case B, c) temperature tendency for case C and d) water vapour tendency for case C. This figure is available in colour online at www.interscience.wiley.com/qj

clearly seen in these plots with the sub-period definitions for case B applicable for the NWP rainfall. Also clear in these plots is the behaviour of the NWP model as it progresses in its forecast cycle. Both the dynamics and the rainfall produced show a significant 'spin-down' in the NWP model. By spin-down we mean the dynamics is very active during the early stages of the forecast (0–24 hours) but reduces quickly as the forecast progresses (24–48 hours). This is clear in both the large-scale tendencies and the surface rain rate, which are both several times larger in the 0–24 hour forecast period.

This spin-down in the NWP model is likely to be a response of the dynamics and physical parametrizations in the model to the analysis used to initialise the model. It can be related to either the quality of the analysis or the parametrizations themselves. It is an important issue to understand but clearly one with strong dynamical feedbacks (a type D2 bias in Table I). An SCM may be able to shed some light on this aspect through sensitivity studies (an area for further work within the Met Office) but the basic comparison of the SCM with the CRM is not sufficient, as the SCM does not allow dynamical feedbacks. It should be noted that ERA-40 causes 'spin-down' of many NWP models and for this reason an interim-reanalysis is currently underway. At the time of this work this was not available but it will be shown in the following section that the spin-down issue does not prevent consistent biases forming in the NWP model and SCM.

4. An investigation of biases in the SCM and NWP model

In this section we look at some examples of the different types of biases described in Table I. As stated previously, a bias is defined as a robust and significant difference between the SCM or NWP model and observations (and/or the CRM depending on which is most suitable). What is meant by significant and robust is somewhat arbitrary but here by robust we mean it is clearly visible in the sub-period averages. By significant we mean that through our scientific insight and knowledge of the model parametrizations we believe that correcting the bias would have a measurable impact on the model performance. The discussion of biases are separated into those that are seen in both the SCM and NWP model (type S) and those that are not (type D). The main focus

DOI: 10.1002/qj

is on those seen in both the SCM and NWP model as these biases are best studied in this framework.

4.1. Examples of similar bias in the SCM and NWP model

Figure 9 shows profiles of the lower troposphere relative humidity averaged over the active and suppressed sub-periods from the NWP model, the SCM, the CRM and observations as processed by Ciesielski *et al*. (2003). A key point to note here is that there is a significant difference in the humidity structure up to 600 m in the CRM and observations depending on whether there is strong convective activity or not. During the suppressed periods, in the CRM and observations, there is a larger increase in humidity over the lower 600 m (approximately 10%) whereas during the active period the increase is notably less (approximately 6%). This response to the convective activity is not seen in either the NWP model or the SCM with a similar increase in humidity of (approximately 15%) in both active and suppressed conditions. The good agreement in this bias between the SCM and NWP model suggests that the SCM is a good tool to investigate this further.

A detailed analysis of the boundary layer structures in the CRM allows us to better understand the reason for different profiles during the active and suppressed phase. By classifying each CRM column as coldpool or not based on temperature difference from the mean, we can see quite different structures in coldpool and non-coldpool regions. For the plots used here, a coldpool is defined as air 0.5 K colder than the domain mean at that level in a contiguous region with a horizontal size greater than 10 km to a height of at least 75 m. However, the features discussed are not sensitive to the exact values used in this definition. Figure 10a shows the different humidity profiles in and out of coldpool columns averaged over the whole of period B. Clearly there are quite different structures in and out of the coldpool regions showing a similar difference to that seen between active and suppressed periods. Figure 10b shows the time series of the fractional area of the domain taken up by coldpools and this confirms that during the active period coldpools columns can make a significant contribution to the total domain mean. This suggests that there may be deficiencies in the representation of the impact of coldpools on the boundary layer in the NWP model and as the coldpools are most likely caused by downdraughts from deep convection the role of both the boundary layer scheme and deep convection scheme are likely to be important. Further work to address this is on-going and will be reported in the literature in some detail at a later date.

It is also worth discussing the differences between the CRM results and the observations. The focus of the discussion above was on structure rather than absolute values, and for the region below 600 m, the observations and the CRM have similar structures and these were significantly different from the SCM and NWP models. However, it is clear that there are also notable differences between the CRM and the observations. In particular the CRM is less humid throughout the profile with the largest differences above 600 m. Differences between the CRM and the observations may be due to imbalances in the forcing data as discussed in Wu *et al*. (2000) or due to deficiencies in the CRM. This issue is not considered any further here but is an example of where the multi-model comparison can add value. Analysis of the other CRMs involved in the comparison shows that all are drier than the observations for the active periods but the Met Office model is one of the driest (Woolnough, personal communication).

A second example of a bias, which can be seen in both the SCM and NWP models, is a positive bias in relative humidity over a region close to convection top with a negative bias below this. Figure 11 shows the relative humidity in the mid- and upper- troposphere averaged over the active period of case B. During this period convection was generally reaching between 12 and 14 km in the SCM, and 13 and 15 km in the NWP model (not shown). When the SCM is compared against the CRM, and the NWP model is compared against observations, the bias is clear with the different heights

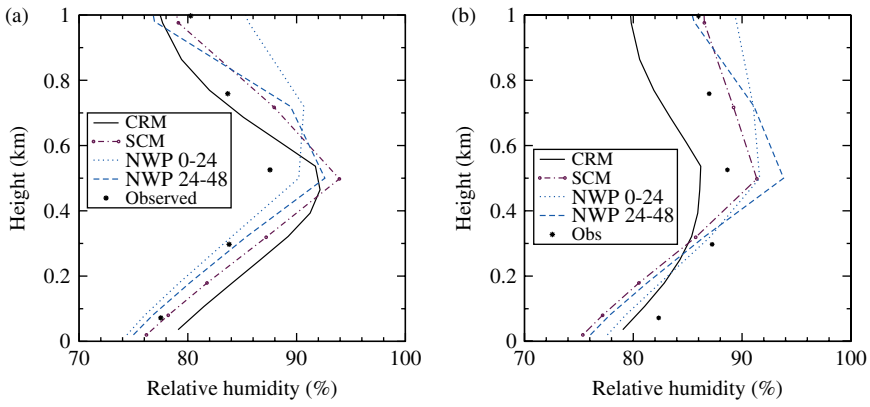

Figure 9. Lower troposphere relative humidity profiles averaged over the a) suppressed and b) active sub-periods for case B. Shown are results from the two forecast periods of the NWP model, the SCM and the CRM. Also included are observations. This figure is available in colour online at www.interscience.wiley.com/qj

DOI: 10.1002/qj

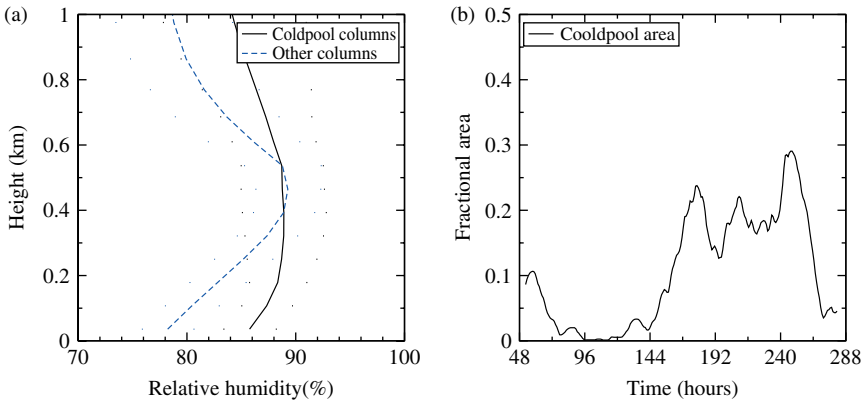

Figure 10. Show in a) is the lower troposphere relative humidity profiles from the CRM for case B averaged for coldpool and non-coldpool regions of the domain through the entire of case B. Shown in b) is the time series of the fractional area occupied by coldpools. A coldpool is defined as air 0.5 K colder than the domain mean at that level in a contiguous region with a horizontal size greater than 10 km to a height of at least 75 m. This figure is available in colour online at www.interscience.wiley.com/qj

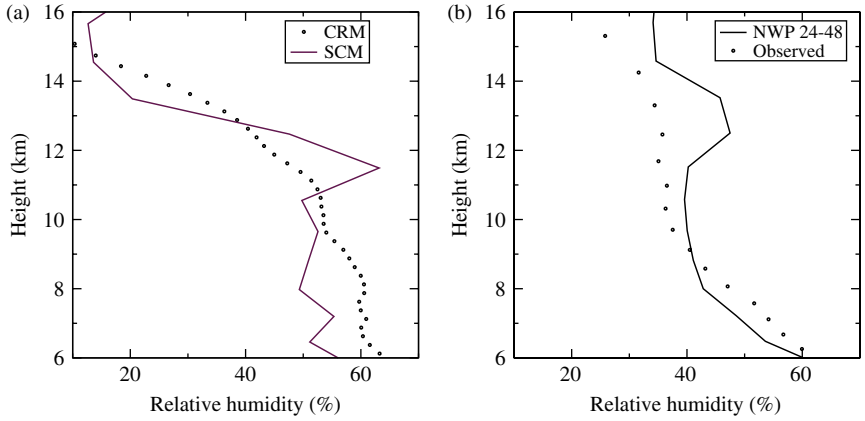

Figure 11. Relative humidity profiles in the mid- and upper- troposphere for the active period of case B. Show is a) a comparison of the CRM and SCM and b) a comparison of the NWP model for the 24–48 hour forecast period and the observations. This figure is available in colour online at www.interscience.wiley.com/qj

of the bias in the SCM and NWP model associated with the different convection tops. As this bias is associated with the convection top it is best to use the CRM rather than observations to define this bias in the SCM as they both use the same forcing and therefore have the convection reaching a very similar height. Using the SCM for Case C provides an even clearer link between the convection top and this relative humidity bias because it had a period of several days of slowly deepening convection. Figure 12a shows the relative humidity in the SCM differenced from the CRM with a solid line showing the height of convection top in the SCM. It can be seen that the SCM is significantly more humid in the region of its convective top and less humid below this as the convection top increases from 5 km to 13 km.

The humidity bias around the top of convection has been linked to a sharp decrease in mass flux in this region (see Figure 13b) and changes to the convection scheme have been made to address this. These changes (discussed in detail in Maidens and Derbyshire, 2007) replace the current condition, which forces detrainment when the plume buoyancy drops below a fixed threshold, with a scheme in which the buoyancy threshold depends on the rate at which plume buoyancy decreases with height. The impact of these changes in the context of the bias discussed here can be seen in Figure 12b, which is the same as Figure 12a but uses the changed convection scheme. It is clear that while there is still a small positive humidity bias in the region of the convection top the size of the bias is significantly reduced.

4.2. Examples of biases not in both the SCM and NWP model

For this experiment, the dominant bias, which cannot be seen in both the SCM and NWP model, is the spin-down issue; this has been discussed in some detail in Section 3 but it warrants further discussion here. Figure 13 shows further details of how the NWP model changes through the forecast cycle and how the SCM is unable to demonstrate this response. Figure 13 shows the mean Q1 (using the standard definition) and convective mass flux from the NWP model, SCM and CRM. For this example, the SCM has been run daily as 48-hour forecasts so it

DOI: 10.1002/qj

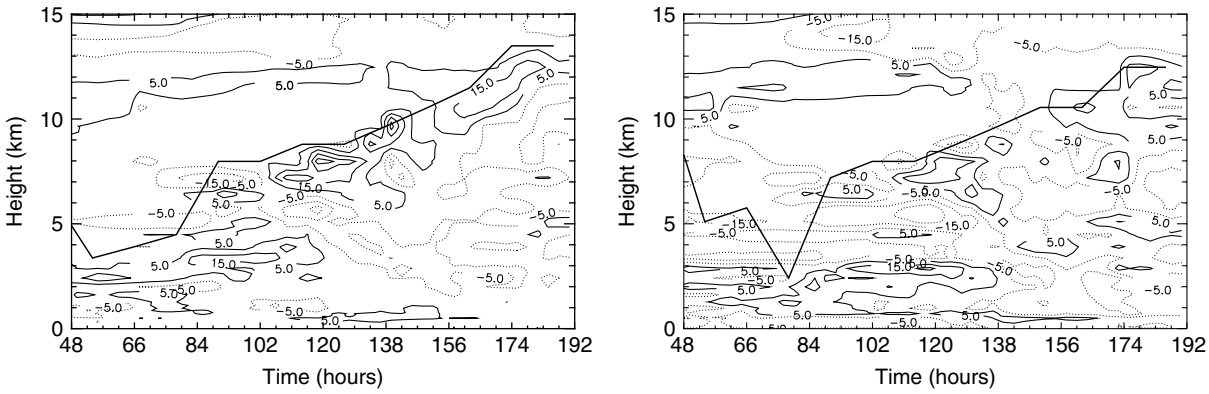

Figure 12. Time-height plots for case C showing the difference in relative humidities from the CRM for a) the standard SCM and b) a version of the SCM with a modified convection scheme. The contour interval is 5% humidity, also included is a line showing the 12-hourly mean height of the convection top in the SCM.

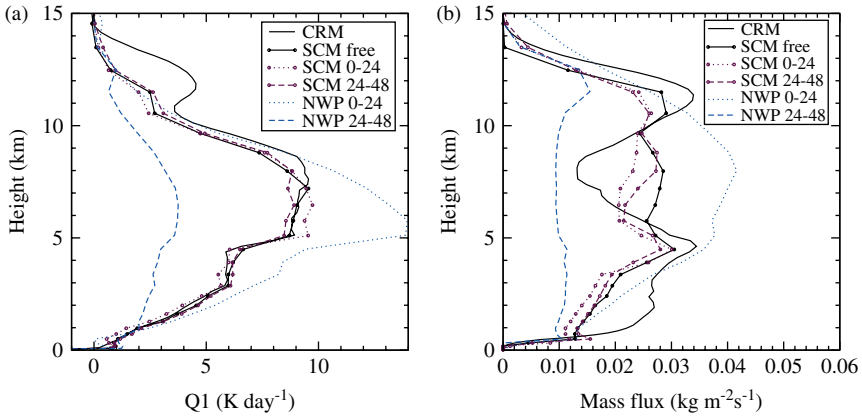

Figure 13. Time mean profiles of a) Q1 and b) convective mass flux from the active period of for case B defined in Table II. This figure is available in colour online at www.interscience.wiley.com/qj

can be cleanly compared to the NWP model. The spin-down in the NWP model is very evident but there is little evidence of any such behaviour in the SCM. As there was very little difference between the observations and analysis for case B this confirms that the 'spin-down' seen in the NWP model is dominated by dynamical feedbacks. The SCM may be useful to better understand the role of the parametrizations in this process but compared to the 'type S' bias it will be far less straightforward to link the SCM results to the behaviour of the full NWP model.

The issue of spin-down in the Met Office NWP model is likely to be strongly linked to the use of ERA-40 and this will be investigated further with this framework when a new analysis is released. Even with the current analysis, this is an example where the intercomparison of different NWP models will add a great deal of value as it can highlight how different models evolve through a forecast period; this is work in progress within the GCSS PCSWG. Sensitivity studies with an SCM may also be able to help understand the link between the analysis and the dynamical response of the NWP model. For example, a comparison of the early behaviour of the physical parametrizations in an SCM initialised with a range of initial conditions may help us understand the relationship between the initial conditions and the response of the parametrizations that influence the dynamics in the full NWP model.

Biases seen only in the SCM (type D1 in Table I) could also be seen in this simulation. For example, the SCM had a warm bias in the mid-troposphere during the suppressed periods that was not seen in the full NWP model. Also, the convection cloud top was seen to be too low in the SCM when compared to the CRM but this was not seen in the full NWP model. However, none of these warrant discussion here as they were either not very large or cannot be linked to significant known problems in the full model.

5. Summary

This paper describes the design and basic results from a new case study involving the comparison of a CRM, an SCM and an NWP model. Each model is used to simulate periods that include a sub-period of strong convective activity and a more suppressed sub-period. The CRM and SCM were forced using data derived from observations taken during TOGA-COARE. The NWP model was initialised daily using ERA-40 and run through a 48-hour forecast cycle with the analysis of results carried

DOI: 10.1002/qj

out over the same region of the TWP that the CRM and SCM forcing represented. The design of this case and the basic results have been presented in some detail as it is a new strategy to involve all these model types in a single study. The design of this experiment is also important as it is currently being used for a multi-model comparison being carried out by the GCSS PCSWG. It is hoped that the basic findings presented here, and any subsequent papers describing the multi-model comparisons, will be a useful framework for any centre involved in the testing and development of parametrizations in NWP or climate models.

As the SCM and CRM were driven using forcing derived directly from local observations and the NWP model was initialised from a global analysis it was far from clear whether the behaviour of these models would be similar. This was the first question addressed in this study. It was found that of the two periods tested, with durations of 8 and 10 days, only one period was very similar in both the NWP model and the CRM. The other period differed because the convectively active sub-period seen in the observations, CRM and SCM, was not seen in the NWP model. This meant that while both periods could be used for comparison of the SCM with the CRM, only one was appropriate for comparison between the NWP model and the SCM/CRM. The lack of convection in the NWP model for one of the selected periods was associated with significantly drier conditions in the analysis than in the observations but the cause of this was not investigated further within this paper.

The paper then focused on the period that had good agreement between the analysis and the observations and discussed where the SCM and NWP model had similar behaviours and where they differed. Examples of where the SCM exhibited a similar bias to that seen in the full NWP model were in the thermodynamic structure of the boundary layer during active convection and in relative humidity in the region of the convection top. For these examples it was suggested that the SCM was a good tool to evaluate this problem in more detail. For the bias in the boundary layer structure further analysis of the CRM was used to link this bias to the representation of coldpools. For the humidity structure near cloud top, a change to the method of calculation detrainment in the convective parametrization was shown to reduce the bias.

Examples of biases seen in the NWP model but not seen in the SCM were dominated by the 'spin-down' during the forecast cycle. This spin-down was shown to be a strongly dynamical response of the model to the analysis used. It was not clear how basic analysis of the SCM within this framework could help to address this issue. It may be the case that experiments could be designed with an SCM that could help to understand the role of the parametrizations in the spin-down process but interpretation of these results will be difficult without support from the full model.

While specific examples were discussed, the main goal of this paper was to describe a basic case study that can be used to address parametrization issues in NWP and climate models. This can either be through individual centres carrying out this case or through comparison of several models of each type as is ongoing within the GCSS PCSWG. There will be significant value from a multi-model comparison using this framework. Multiple CRMs will provide additional confidence and a measure of uncertainty for any diagnostic used to identify biases in the SCM and NWP models. A comparison of different NWP models may help address further issues such as to what extent the spin-down in an NWP model is related to the analysis, and to what extent it is related to its parametrizations. Also with multiple SCMs and NWP models, biases for this case can be identified as either a community-wide problem or a problem specific to one model. For biases that are specific to one model, understanding and ideas to address the bias can often be gained from careful analysis of the models without the bias.

Acknowledgements

This work has been designed and coordinated within the GCSS framework, so Christian Jakob as its chair and all members of the GCSS scientific steering group have played a role in leading us to a study of this kind. The multi-model comparison work using this case study is on-going and contributions to this comparison have helped focus aspects of this paper. Therefore it is important to acknowledge all participants involved in the current GCSS PCSWG case study (see www.convection.info). Specifically for discussions about this paper Jon Petch would like to thank Andy Brown, Adrian Lock, Roy Kershaw, Peter Bechtold and Steve Klein. Also two anonymous reviewers added value to this paper through very helpful comments.

References

Bechtold P, Redelsperger JL, Beau I, Blackburn M, Brinkop S, Grandpeix JY, Grant A, Gregory D, Guichard F, Hoff C, Ioannidou E. 2000. A GCSS model intercomparison for a tropical squall line observed during TOGA-COARE. II: Intercomparison of single-column models and a cloud-resolving model. *Q. J. R. Meteorol. Soc.* **2000**: 865–888.

Brown AR, Derbyshire SH, Mason PJ. 1994. Large-eddy simulation of stable atmospheric boundary layers with a revised stochastic subgrid model. *Q. J. R. Meteorol. Soc.* **120**: 1485–1512.

Brown PRA, Heymsfield AJ 2001. The microphysical properties of tropical convective anvil cirrus: A comparison of model and observations. *Q. J. R. Meteorol. Soc.* **127**: 1535–1550.

Ciesielski PE, Johnson RH, Haertel PT, Wang J. 2003. Corrected TOGA COARE sounding humidity data: Impact on diagnosed properties of convection and climate over the warm pool. *J. Climate* **16**: 2370–2384.

Edwards JM, Slingo A. 1996. Studies with a flexible new radiation code. Part I. Choosing a configuration for a large-scale model. *Q. J. R. Meteorol. Soc.* **122**: 689–719.

Grabowski WW, Bechtold P, Cheng A, Forbes R, Halliwell C, Khairoutdinov M, Lang S, Nasuno T, Petch J, Tao WK, Wong R, Wu X, Xu KM. 2005. Daytime convective development over land: a model intercomparison based on LBA observations. *Q. J. R. Meteorol. Soc.* **132**: 317–344.

Grabowski WW. 2003. Impact of ice microphysics on multiscale organization of tropical convection in two-dimensional cloud-resolving simulations. *Q. J. R. Meteorol. Soc.* **129**: 67–81.

Gregory D, Miller MJ. 1989. A numerical study of the parametrization of deep tropical convection. *Q. J. R. Meteorol. Soc.* **115**: 1209–1241.

Inness PM, Slingo JM, Woolnough SJ, Neale RB, Pope VD. 2001. Organisation of tropical convection in a GCM with varying vertical resolution; Implications for the Simulation of the Madden-Julian Oscillation. *Climate Dyn.* **17**: 777–793.

Johnson RH, Rickenbach TM, Rutledge SA, Ciesielski PE, Schubert WH. 1999. Trimodal characteristics of tropical convection. *J. Climate* **12**: 2387–2418.

Klein SA, Jiang X, Boyle J, Malyshev S, Xie S. 2006. Diagnosis of the summertime warm and dry bias over the U.S. Southern Great Plains in the GFDL climate model using a weather forecasting approach. *Geophys. Res. Lett.* **33**: L18805 doi:10.1029/2006GL027567.

Lin X, Johnson RH. 1996. Heating, moistening and rainfall over the Western Pacific Warm Pool during TOGA-COARE. *J. Atmos. Sci.* **53**: 3367–3383.

Maidens AV, Derbyshire SH. 2007. Improving mass flux profiles in the Gregory-Rowntree convection scheme using adaptive detrainment. *Q. J. R. Meteorol. Soc.* submitted **1**: 21.

Martin GM, Ringer MA, Pope VD, Jones A, Dearden C, Hinton TJ. 2005. The physical properties of the atmosphere in the new Hadley Centre Global Environment Model (HadGEM1). Part I: model description and global climatology. *J. Climate* **19**: 1274–1301.

Petch JC, Gray MEB. 2001. Sensitivity Studies Using a Cloud Resolving Model Simulation of the Tropical West Pacific. *Q. J. R. Meteorol. Soc.* **127**: 2385–2394.

Randall DA, Xu K-M, Sommerville RJC, Icobellis S. 1996. Single-column models and cloud ensemble mdels as links between observations and climate models. *J. Climate* **9**: 1683–1697.

Randall DA, Curry J, Duynkerke P, Krueger S, Miller M, Ryan B, Starr D, Rossow W, Tselioudis G, Wielicki B. 2000. The Second GEWEX Cloud System Study Science and Implementation Plan. *IGPO Publication Series* **34**: 45 pp.

Redelsperger JL, Brown P, Guichard F, Hoff C, Kawasima M, Lang S, Montmerle Th, Nakamura K, Saito K, Seman C, Tao W-K, Donner LJ. 2000. A GCSS model intercomparison for a tropical squall line observed during TOGA-COARE. Part 1: Cloud-Resolving Models. *Q. J. R. Meteorol. Soc.* **126**: 823–864.

Redelsperger JL, Parsons DB, Guichard F. 2002. Recovery processes and factors limiting cloud-top height following the arrival of a dry intrusion observed during TOGA COARE. *J. Atmos. Sci.* **59**: 2438–2457.

Shutts GJ, Gray MEB. 1994. A numerical modelling study of the geostrophic adjustment process following deep convection. *Q. J. R. Meteorol. Soc.* **120**: 1145–1178.

Swann H. 1998. Sensitivity to the representation of precipitating ice in CRM simulations of deep convection. *Atmos. Res.* **47–48**: 415–435.

Uppala SM, Kallberg PW, Simmons AJ, Andrae U, Bechtold VD, Fiorino M, Gibson JK, Haseler J, Hernandez A, Kelly GA, Li X, Onogi K, Saarinen S, Sokka N, Allan RP, Andersson E, Arpe K, Balmaseda MA, Beljaars ACM, Van De Berg L, Bidlot J, Bormann N, Caires S, Chevallier F, Dethof A, Dragosavac M, Fisher M, Fuentes M, Hagemann S, Holm E, Hoskins BJ, Isaksen L, Janssen PAEM, Jenne R, McNally AP, Mahfouf JF, Morcrette JJ, Rayner NA, Saunders RW, Simon P, Sterl A, Trenberth KE, Untch A, Vasiljevic D, Viterbo P, Woollen J. 2005. The ERA-40 re-analysis. *Q. J. R. Meteorol. Soc.* **131**: 2961–3012.

Webster PJ, Lukas R. 1992. TOGA COARE: The Coupled Ocean Atmosphere Response Experiment. *Bull. Am. Meteorol. Soc.* **73**: 1377–1416.

Wu X, Moncreiff MW, Emanuel KA. 2000. Evaluation of Large-Scale Forcing during TOGA COARE for Cloud-Resolving Models and Single-Column Models. *J. Atmos. Sci.* **57**: 2977–2985.

Xie S, Xu K-M, Cederwall RT, Bechtold P, Del Genio AD, Klein SA, Cripe DG, Ghan SJ, Gregory D, Iacobellis SF, Krueger SK, Lohmann U, Petch JC, Randall DA, Rotstayn LD, Somerville RCJ, Sud YC, von Salzen K, Walker GK, Wolf A, Yio JJ, Zhang GJ, Zhang M. 2002. Intercomparison and evaluation of cumulus parameterizations under summertime midlatitude continental conditions. *Q. J. R. Meteorol. Soc.* **128**: 1095–1136.

Xu K-M, Cederwall RT, Donner LJ, Grabowski WW, Guichard F, Johnson DE, Khairoutdinov M, Krueger SK, Petch JC, Randall DA, Seman CJ, Tao W-K, Wang D, Xie SC, Yio JJ, Zhang M-H. 2002. An intercomparison of Cloud-Resolving Models with the ARM Summer 1997 IOP data. *Q. J. R. Meteorol. Soc.* **128**: 593–624.

Zhang MH, Lin JL. 1997. Constrained variational analysis of sounding data based on column-integrated budgets of mass, heat, moisture and momentum: Approach and application to ARM measurements. *J. Atmos. Sci.* **54**: 1503–1524.